Journal of Integrative Agriculture 2026, 25(2): 803–813

Available online at ScienceDirect

Journal of Integrative Agriculture



RESEARCH ARTICLE

A novel TLR7 agonist exhibits antiviral activity against pseudorabies virus

Yue Song[1, 4, 5*], Heng Wang[1, 4, 5*], Mingyang Wang[1, 4, 5*], Yumin Wang[1, 4, 5], Xiuxiang Lu[1, 4, 5], Wenjie Fan[1, 4, 5], Chen Yao[1, 4, 5], Pengxiang Liu[1, 4, 5], Yanjie Ma[1, 4, 5], Shengli Ming[1, 4, 5], Mengdi Wang[2#], Lijun Shi[3#]

[1] *College of Veterinary Medicine, Henan Agricultural University, Zhengzhou 450046, China*
[2] *College of Food and Bioengineering, Henan University of Animal Husbandry and Economy, Zhengzhou 450046, China*
[3] *College of Sciences, Henan Agricultural University, Zhengzhou 450046, China*
[4] *Key Laboratories of Animal Biochemistry and Nutrition, Ministry of Agriculture and Rural Affairs, Zhengzhou 450046, China*
[5] *Key Laboratory of Animal Growth and Development of Henan Province, Zhengzhou 450046, China*

Highlights

- A novel TLR7 agonist (a pyrrolo[3,2-*d*]pyrimidine derivative, named TLR713) exhibits antiviral activity against PRV *in vitro* and *in vivo*.
- TLR713 specifically inhibits PRV replication but does not affect viral attachment, entry, assembly or release.
- TLR713 shows low cytotoxicity and might be potential antiviral agents for being tested clinically.

Abstract

Innate immunity is the primary defense against viral infections, with Toll-like receptors (TLRs) playing a crucial role in this process. This study aims to highlight the effectiveness of a pyrrolo[3,2-*d*]pyrimidine derivative (named TLR713), a potential TLR7 agonist, in inhibiting pseudorabies virus (PRV) replication both *in vitro* and *in vivo*. Tests on PK-15 cells demonstrated that TLR713 had no significant impact on cell viability, cell cycle progression, or apoptosis at concentrations of 0–3 μmol L^{-1}. TLR713 could promote the phosphorylation of IκBα, p38, and JNK through TLR7, and increase the expression of inflammatory cytokines. *In vitro*, when cells were treated with TLR713, PRV proliferation was inhibited *via* TLR7 pathway. Analysis of the viral life cycle indicated that TLR713 could inhibit the replication of PRV, but not affect viral attachment, entry, assembly, or release. *In vivo*, TLR713 showed no side effects on mice at a concentration of 25 mg kg^{-1}. It improved the survival rate of PRV-infected mice, reduced tissue viral load, and alleviated the inflammatory response. In summary, this study highlights the potential of TLR713 as a novel TLR7 agonist capable of inhibiting PRV replication and may offer new opportunities for developing antiviral therapies.

Keywords: Toll-like receptors, TLR7 agonist, innate immunity, antiviral effect

1. Introduction

Immune responses are crucial in protecting humans and animals against viral infections (Koerner *et al.* 2021). With the immune system, pathogen-associated molecular patterns (PAMPs) of fungi, bacteria, and viruses can be detected by pattern recognition receptors (PRRs) to trigger innate immune responses aimed at eliminating the threat (Xiao *et al.* 2014; Shao *et al.* 2020), including Toll-like receptors (TLRs) (Jahanban-Esfahlan *et al.* 2019; Fernandes-Santos and Azeredo 2022). TLRs which are widely expressed, recognize pathogens, and serve as the initial defense line within the innate immune system (Xun *et al.* 2021). As key innate immune sensors, TLRs not only induce cytokine production but also enhance capacities for phagocytosis, microbicidal activity, and antigen presentation (Mentrup *et al.* 2022). TLRs recognize various PAMPs containing nucleic acids,

Received 31 October 2023; Received in revised form 5 March 2024; Accepted 22 April 2024; Available online 4 July 2024
Yue Song, E-mail: songyue2008@163.com; Heng Wang, E-mail: wanghheng9264@163.com; Mingyang Wang, E-mail: 2595684085@qq.com; #Correspondence Mengdi Wang, E-mail: mengdi.ok@163.com; Lijun Shi, E-mail: shilijunpku@126.com
*These authors contributed equally to this study.

© 2026 CAAS. Publishing services by Elsevier B.V. on behalf of KeAi Communications Co. Ltd. This is an open access article under the CC BY-NC-ND license (http://creativecommons.org/licenses/by-nc-nd/4.0/). Peer review under responsibility of Editorial Board of *Journal of Integrative Agriculture*.
doi: 10.1016/j.jia.2024.07.001

initiate signaling cascades, and provoke immune responses (Naqvi *et al.* 2022). The TLR family is divided into two major categories: surface TLRs and intracellular endosomal TLRs. Surface TLRs, located on the plasma membrane, bind to microbial ligands, whereas intracellular endosomal TLRs, found on the endosomal membrane, are sensitive to DNA/RNA from pathogens (Takeda and Akira 2004).

TLR7 is a member of the TLR family and is an endosomal single-stranded RNA (ssRNA) sensor that initiates innate immune responses during viral and bacterial infections (Yeh *et al.* 2023). TLR7 has two loading sites: a Guanosine-loaded site and an ssRNA-loaded site (PDB code: 5GMF) (Zhang *et al.* 2016). According to published reports, a TLR7 agonist typically binds near the Guanosine-loaded site to perform its function (PDB code: 5GMF, 6IF5, 5ZSA, etc.). Compounds such as R837 and R848 can bind to TLR7 near the Guanosine-loaded site to activate TLR7. When TLR7 is activated by compounds and/or ssRNA, it triggers a signaling cascade (Vanwalscappel *et al.* 2018). TLR7-mediated signaling primarily operates through the myeloid differentiation primary-response protein 88 (MyD88)-dependent pathway. The messengers in the signaling pathway activate various transcription factors, including nuclear factor kappa-light-chain-enhancer of activated B cells (NF-κB), Jun N-terminal kinase (JNK) etc. (Das *et al.* 2017), which induces the production of proinflammatory cytokines, chemokines, and type I interferon (IFN) (Nishii *et al.* 2018). Many IFNs and pro-inflammatory cytokines have been confirmed to have direct antiviral effects, such as against the hepatitis B virus (HBV) (Lucifora *et al.* 2018).

The innate immune response derived by TLR7 agonists plays a crucial role in modulating viral infections. The use of TLR agonists as antiviral agents has proven to be effective. For instance, TLR1/2, TLR3, and TLR7/8 agonists can inhibit the replication of HBV (Lucifora *et al.* 2018; Janovec *et al.* 2020). In a woodchuck model of chronic hepatitis B, administration of the TLR7 agonist GS-9620 led to a significant reduction of woodchuck hepatitis virus in serum (Menne *et al.* 2015). Imidazoquinolines, such as the TLR7/8 agonist R848 (resiquimod), have been used to treat genital herpes simplex virus type 2 lesions and psoriasis (Mark *et al.* 2007; Gotovtseva *et al.* 2008). Moreover, R848 can also strongly inhibit Zika virus replication (Savidis *et al.* 2016; Vanwalscappel *et al.* 2018), indicating its potential as a therapeutic agent.

Here, we investigated the antiviral effects of a newly developed TLR7 agonist named TLR713, using pseudorabies virus (PRV) as a model virus. TLR713 is a pyrrolo[3,2-*d*] pyrimidine derivative synthesized in our laboratory (Song *et al.* 2024). Through test *in vitro*, we determined that TLR713 effectively inhibits PRV replication by activating innate immunity through TLR7. We confirmed the safety of TLR713 in mice and found that it can also effectively reduce PRV proliferation *in vivo*. Overall, this study confirmed that TLR713 inhibits PRV replication both *in vitro* and *in vivo* and highlights its potential as a therapeutic agent for viral infections.

2. Materials and methods

2.1. Cells, viruses, and plasmids

Porcine kidney epithelial PK-15 cells (CCL-33; ATCC, MD, USA) were grown in monolayers at 37°C under 5% CO_2 in DMEM (10566-016; Gibco, NY, USA) supplemented with 10% FBS (10099141C; Gibco, MA, USA), 100 U mL^{-1} penicillin, and 100 mg mL^{-1} streptomycin sulfate (B540732; Sangon, Shanghai, China). $TLR7^{-/-}$ PK-15 cells were used as previously described (Meng *et al.* 2022). Briefly, CRISPR-Cas9 technology was used to generate $TLR7^{-/-}$ PK-15 cells. PK-15 cells were infected with lentiviruse, selected with puromycin (4 mg mL^{-1}), obtained by serial dilution, and verified by Sanger sequencing and immunoblotting analysis.

The recombinant PRV-GFP strain, derived from the PRV Hubei strain with TK gene replaced by a GFP expression cassette, was kindly donated by Hanzhong Wang from Wuhan Institute of Virology, Chinese Academy of Sciences. The virulent PRV isolate QXX (PRV-QXX) was kindly donated by Yongtao Li (Henan Agricultural University, China). Viral titers were determined using the $TCID_{50}$ assay, which was calculated *via* the Reed-Muench method.

2.2. Mice

Female 6- to 8-wk-old C57BL/6 mice were purchased from the Center of Experimental Animals of Zhengzhou University, China and maintained in a specific pathogen-free animal facility.

2.3. Cell viability assay, cell cycle analysis, and apoptosis analysis

PK-15 cells were seeded into plates and cultured overnight. Next day, the medium was changed with TLR713 (0–10 μmol L^{-1}), and the cells were cultured for another 36 h. The cell viability was evaluated by Cell Counting Kit-8 (CCK-8) assay. The cell cycle was assessed with PI staining in flow cytometry. Apoptosis was assessed with Annexin V-FITC and PI staining in flow cytometry.

2.4. qRT-PCR

Total RNA was extracted using Trizol reagent (9108; TaKaRa, Japan) and reverse transcribed with a PrimeScript RT Reagent Kit (RR047A; TaKaRa). qRT-PCR was performed in triplicate using SYBR Premix *Ex Taq* (RR820A; TaKaRa). Data were normalized to *β-actin*. The relative changes were calculated using the $2^{-\Delta\Delta CT}$ method.

Quantification of the genome copy number of PRV was performed as previously described (Wang *et al.* 2020). Briefly, the PCR product of *PRV-gH* gene (187 bp) was cloned into pGEM-T vector. A standard curve was prepared from serial 10-fold dilutions of the plasmid for the quantification of PRV genome copy number. The primers used for qRT-PCR analysis were described in Appendix A. Each assay was performed in triplicate.

2.5. Immunoblotting analysis

Cells were lysed in RIPA buffer (P0013B, Beyotime, Biotech Inc., Shanghai, China) supplemented with a protease and phosphatase inhibitor cocktail (HY-K0010 and HY-K0022;

MedChemExpress). Protein samples were separated by SDS-PAGE and transferred to polypropylene fluoride membranes (C3117; Millipore). After 30 min incubation in 5% nonfat milk (A600669; Sangon Biotech, Shanghai, China), the membrane was incubated with the primary antibody overnight at 4°C, then incubated with the appropriate HRP-conjugated secondary antibody for 1 h at room temperature. The target proteins were detected with Luminata Crescendo immunoblotting HRP substrate (WBLUR0500; Millipore) on a GE AI600 imaging system (GE Healthcare, Technologies Inc., Chicago, USA). Each assay was performed in triplicate.

2.6. Immunofluorescence analysis

Cells grown on coverslips were fixed with 4% paraformaldehyde in PBS for 30 min at room temperature. Then cells were nonpermeabilized or permeabilized with 0.2% Triton X-100 for 20 min, blocked with PBS containing 10% FBS for 1 h at room temperature, washed three times with PBS and incubated with the PRV-gB antiserum for 1 h at room temperature. Cells were then incubated with the appropriate Alexa-Fluor-conjugated secondary antibodies for 1 h at room temperature. The images were captured using a Zeiss LSM 800 confocal microscope (Oberkochen, Germany). Each assay was performed in triplicate.

2.7. Viral attachment, entry, assembly and secretion assay

Viral attachment assay Cells were incubated with PRV-QXX with or without TLR713 (1 μmol L^{-1}) at 4°C for 1 h. After three extensive washes with ice-cold PBS, viral attachment assays were performed by immunofluorescence analyses and $TCID_{50}$ analysis.

Viral entry assay Cells were incubated with PRV-QXX at 4°C for 1 h. Cells were extensively washed three times with ice-cold PBS, shifted to 37°C for 30 min with or without TLR713 (1 μmol L^{-1}) to allow entry, washed with trypsin (1 mg mL^{-1}) to remove any residual virions. Viral entry was detected by immunofluorescence analyses and $TCID_{50}$ analysis.

Viral assembly assay Cells were infected with PRV-QXX (MOI=0.1). The efficiency of viral assembly was determined by comparing the infectious titers ($TCID_{50}$ mL^{-1}) with the total PRV genome equivalents (GE).

Viral secretion assay Cells were infected with PRV-QXX (MOI=0.1). The medium was replaced with or without TLR713 (1 μmol L^{-1}) at 12 h after infection, and the supernatants and cells were harvested at 24 h after the medium changed. The infectivity of viral supernatants and cells were determined by $TCID_{50}$ assay. Each assay was performed in triplicate.

2.8. $TCID_{50}$ assay

$TCID_{50}$ assay was performed to quantify the viral titers. Briefly, PK-15 cells grown in a 96-well plate were infected with 10-fold dilutions of PRV-QXX, incubated at 37°C for a further 3–5 d, followed by observing the cytopathic effect of each well under a light microscope. The $TCID_{50}$ was calculated using the Reed-Muench method. Each assay was performed in triplicate.

2.9. Mice experiments

Female 6- to 8-wk-old C57BL/6 mice were purchased from the Center of Experimental Animal of Zhengzhou University (Zhengzhou, China) and maintained in a specific-pathogen-free animal facility. Sacrifice was performed with isoflurane narcosis.

2.10. Statistical analysis

Data are representative of at least three independent experiments for quantitative analyses. All statistical analyses were performed with a two-tailed Student's *t*-test. Significant differences relative to the corresponding controls were accepted at $P<0.05$.

3. Results

3.1. Effects of TLR713 on cell viability, cell cycle and apoptosis

The structure of TLR713 is shown in Fig. 1-A. TLR713 was synthesized through three-step chemical reactions using 2,4-dichloro-5*H*-pyrrolo[3,2-*d*]pyrimidine, 1-(chloromethyl)-2-methoxybenzene, and *t*-butyl (4-aminobutyl)carbamate as materials (Song *et al.* 2024). To analyze the effects of TLR713 on cell viability, cell cycle, and apoptosis, PK-15 cells were cultured with different concentrations of TLR713 (0–10 μmol L^{-1}). Cell viability was measured using CCK-8 assay. The results indicated that TLR713 at a relatively high concentration (10 μmol L^{-1}) could significantly inhibit cell viability (Fig. 1-B). Further analysis showed that the CC_{50} (median cytotoxic concentration) value of TLR713 on PK-15 cells was 19.886 μmol L^{-1} (Fig. 1-C). The effect of TLR713 on the cell cycle was also analyzed. TLR713 used on PK-15 cells at concentrations of 0–3 μmol L^{-1} resulted in normal cell cycle progression, while at a concentration of 10 μmol L^{-1}, it resulted in cell-cycle arrest in the G1 phase (Fig. 1-D). Additionally, treatment with TLR713 at concentrations of 0–3 μmol L^{-1} for 36 h had no effect on cell apoptosis in PK-15 cells. However, when PK-15 cells were treated with TLR713 at a concentration of 10 μmol L^{-1}, the percentage of apoptotic cells increased significantly (Fig. 1-E). Overall, these findings suggest that treatment with TLR713 at concentrations of 0–3 μmol L^{-1} for 36 h has minimal harmful effects on PK-15 cells.

3.2. TLR713 is a TLR7 agonist

Initially, we assumed TLR7 was the intended target when TLR713 was synthesized. To determine whether TLR713 is a TLR7 agonist, $TLR7^{-/-}$ PK-15 cells were treated with TLR713. Treatment with TLR713 in PK-15 cells greatly increased the expression of interleukin and tumor necrosis factor at the mRNA level, and the mRNA expression levels of downstream interferon and interferon-stimulated genes were also significantly enhanced. However, this phenomenon was not observed in $TLR7^{-/-}$ PK-15 cells (Fig. 2-A). Immunoblotting analyses confirmed the knockout of the TLR7 gene in $TLR7^{-/-}$ PK-15 cells (Fig. 2-B). In $TLR7^{-/-}$ PK-15 cells, TLR713 could not phosphorylate IκBα, p38, and JNK in the TLR7 signaling pathway, whereas the phosphorylation of these molecules was enhanced over time in $TLR7^{WT}$ PK-15 cells (Fig. 2-B).

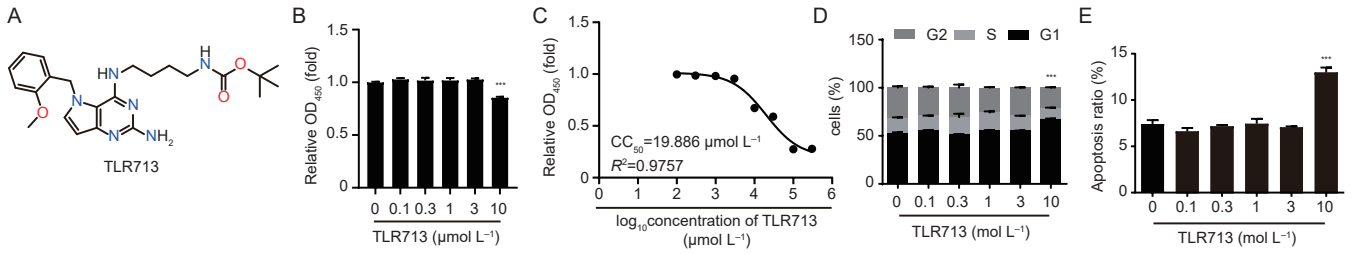


Fig. 1 Effects of TLR713 on cell viability, cell cycle and apoptosis. A, chemical structure of TLR713. B and D, PK-15 cells were treated with TLR713 (0–10 μmol L^{-1}) for 36 h. Cell viability was assessed with CCK-8 assay (B) and cell cycle was assessed with PI staining in flow cytometry (D). C, CC_{50} curves of TLR713 on PK-15 cells. E, PK-15 cells were treated with TLR713 (0–10 μmol L^{-1}) for 36 h. Apoptosis was assessed with Annexin V-FITC and PI staining in flow cytometry, quantification of the percentage of apoptosis cells was shown in E. CC_{50}, half-maximal cytotoxic concentration. Data are mean±SD (*n*=3). ***, *P*<0.001.

Collectively, these data indicate that TLR713 is a TLR7 agonist.

3.3. TLR713 inhibits PRV proliferation through TLR7 pathway *in vitro*

To assess the inhibitory effects of TLR713 on PRV proliferation, a recombinant PRV-GFP strain expressing the GFP reporter was used. Fluorescent microscopy revealed a significant decrease in the GFP signal when cells were treated with TLR713, indicating that TLR713 suppresses PRV-GFP replication (Fig. 3-A and B). To further validate the anti-PRV effect of TLR713, we evaluated its antiviral effects against the PRV-QXX strain. Firstly, viral titration assays showed that TLR713 caused a decrease in PRV-QXX progeny virus production (Fig. 3-C). Then, we used qRT-PCR to analyze the *PRV-gB* gene expression level and found that TLR713 treatment dramatically downregulated *PRV-gB* mRNA transcript in PK-15 cells (Fig. 3-D). Additionally, PRV-gB protein expression was also significantly reduced when PK-15 cells were treated with TLR713 (Fig. 3-E). Overall, these results provide evidence that TLR713 can effectively inhibit PRV proliferation in PK-15 cells.

To determine whether TLR713 inhibits PRV proliferation *via* TLR7, $TLR7^{-/-}$ PK-15 cells were used. Both $TLR7^{-/-}$ and $TLR7^{WT}$ PK-15 cells were treated with TLR713 and then infected with PRV-GFP and PRV-QXX. The analyses of flow cytometry (Fig. 3-F), $TCID_{50}$ (Fig. 3-G) and the expression of PRV-gB (Fig. 3-H) showed that TLR713 inhibited PRV proliferation *via* TLR7. Taken together, these results suggest that TLR713 exerts its anti-PRV effect through the TLR7 pathway.

3.4. TLR713 restricts PRV replication

We next investigated the effect of TLR713 on the PRV life cycle. PK-15 cells were treated with TLR713 and infected with PRV at 4°C for 1 h, were then cultured at 37°C for 24 h without TLR713. The viral titer was measured by $TCID_{50}$ assay (Fig. 4-A). There were no significant differences in viral attachment with or without TLR713. Immunofluorescence assays also showed similar results (Fig. 4-B). To investigate the impact of TLR713 on PRV entry, PK-15 cells were incubated with PRV-QXX on ice for 1 h, shifted to 37°C for 30 min with or without TLR713, then cultured at 37°C for 24 h without TLR713. Viral titer was measured using the $TCID_{50}$ assay. As shown in Fig. 4-C, there were no significant changes in viral entry into PK-15 cells with or without TLR713. Immunofluorescence assays confirmed these results (Fig. 4-D). Additionally, we examined whether TLR713 influenced viral replication. After PRV entry into PK-15 cells, the cells were cultured with TLR713 for another 24 h. Virus proliferation was detected by a virus titer assay (Fig. 4-E), and the expression of the PRV-gB protein was detected by immunoblotting analysis (Fig. 4-F). These results indicated that TLR713 inhibited PRV replication. We also analyzed the effect of TLR713 on viral assembly and release. The results showed that TLR713 had no impact on PRV assembly, as determined by comparing infectious titers with PRV genome equivalents (Fig. 4-G). TLR713 treatment did not alter the infectivity of intracellular and extracellular PRV, suggesting that TLR713 had no effect on viral release (Fig. 4-H). Collectively, these results indicate that TLR7 acts on the replication stage of the PRV life cycle.

3.5. TLR713 does not produce adverse side effects *in vivo*

To assess the antiviral effect of TLR713 *in vivo*, we first evaluated the toxicity of TLR713 on mice (Fig. 5-A). The administration of TLR713 at various doses did not affect the growth or external appearance of the mice, as demonstrated by consistent body weight (Fig. 5-B) and observation. None of the mice receiving TLR713 experienced mortality due to TLR713 exposure. Liver toxicity was assessed by measuring serum alanine aminotransferase (ALT) and aspartate aminotransferase (AST) levels. As shown in Fig. 5-C and D, normal serum ALT and AST levels were observed after 4 consecutive weeks of TLR713 treatment at doses of 5 or 35 mg kg^{-1}, suggesting a lack of significant liver damage. Additionally, macroscopic analysis revealed no histomorphological changes resulting from TLR713 treatment. To investigate the potential toxicity to major organs, H&E staining was utilized, and the results indicated no observable abnormalities or organ damage in any of the experimental groups (Fig. 5-E). These results provide direct evidence that TLR713 exhibits negligible tissue toxicity.

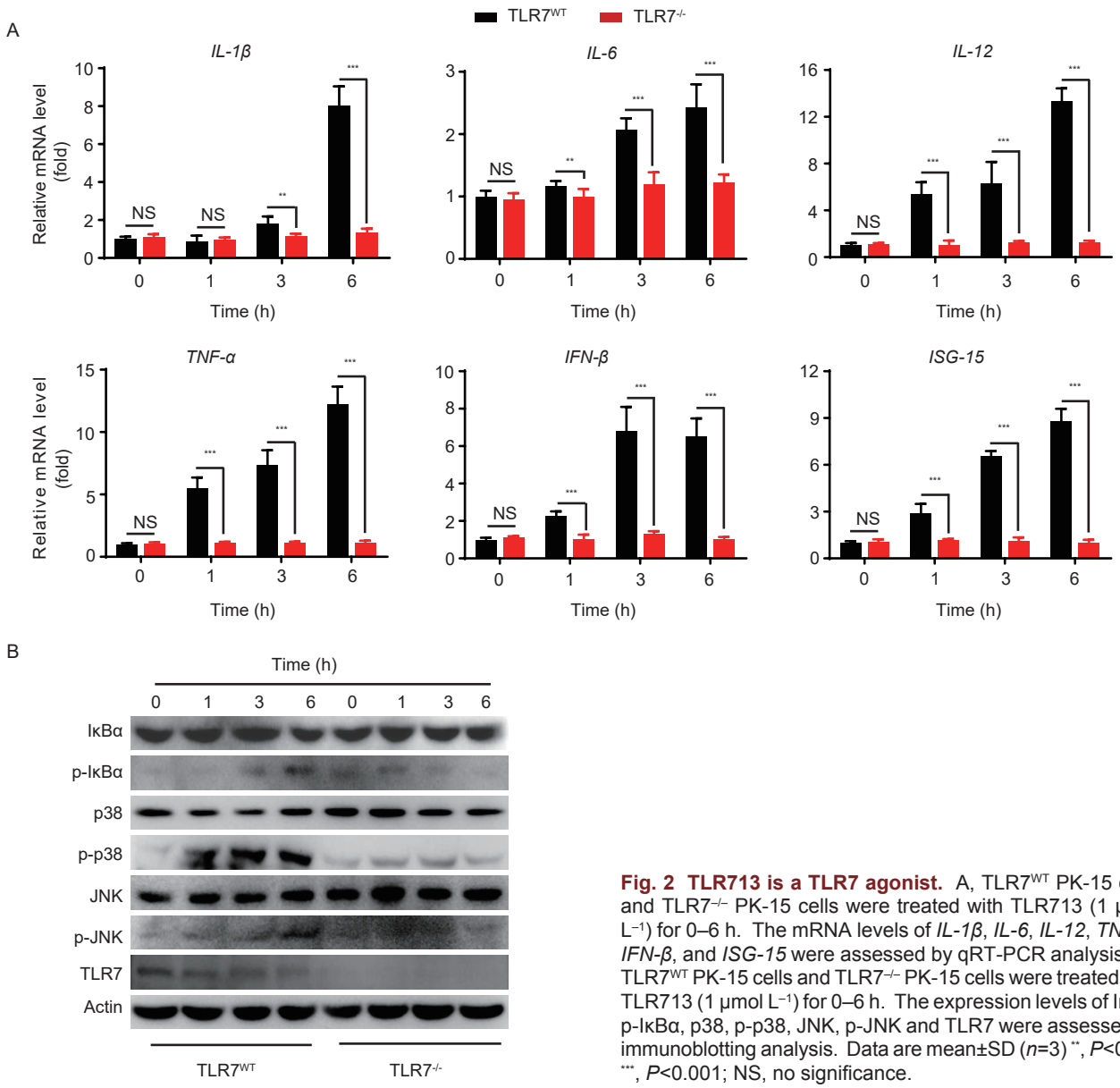


Fig. 2 TLR713 is a TLR7 agonist. A, TLR7^{WT} PK-15 cells and TLR7$^{-/-}$ PK-15 cells were treated with TLR713 (1 μmol L^{-1}) for 0–6 h. The mRNA levels of *IL-1β*, *IL-6*, *IL-12*, *TNF-α*, *IFN-β*, and *ISG-15* were assessed by qRT-PCR analysis. B, TLR7^{WT} PK-15 cells and TLR7$^{-/-}$ PK-15 cells were treated with TLR713 (1 μmol L^{-1}) for 0–6 h. The expression levels of IκBα, p-IκBα, p38, p-p38, JNK, p-JNK and TLR7 were assessed by immunoblotting analysis. Data are mean±SD (n=3) **, P<0.01; ***, P<0.001; NS, no significance.

3.6. TLR713 protects mice against PRV infection

Lastly, the antiviral effects of TLR713 against PRV *in vivo* were investigated (Fig. 6-A). We administered TLR713 in two doses at a concentration of 5 mg kg^{-1} *via* subcutaneous injection on d3 and6 before the PRV-QXX challenge (1×10^3 $TCID_{50}$ per mouse, the median lethal dose). The results showed that TLR713 effectively protected mice from PRV-QXX infection. Upon challenge with 1×10^3 $TCID_{50}$ of PRV-QXX, the expected mortality was observed, with half of the mice dying within 5 days post-infection. In comparison, mice injected with TLR713 exhibited a 75% survival rate during the 7 d observation period (Fig. 6-B). We also examined PRV proliferation in the brain and lung tissues of the infected mice (Fig. 6-C and D). Furthermore, we investigated tissue lesions and inflammatory infiltration in major organs using H&E staining. The mice injected with TLR713 displayed fewer tissue lesions and reduced inflammatory infiltration (Fig. 6-G). qRT-PCR assays revealed lower mRNA level of *IL-6* and *IFN-β* in tissues of mice injected with TLR713 compared to those without TLR713 treatment (Fig. 6-E and F). Overall, our results demonstrate that TLR713 can inhibit PRV infection *in vivo*.

4. Discussion

TLR7 represents a promising target for the design and development of immunomodulators serving as antiviral and anticancer agents, as well as vaccine adjuvants. In recent years, a variety of compounds targeting TLR7 have been developed and confirmed to be useful for antiviral therapy, immune enhancement (Kanneganti *et al.* 2006; Tomai *et al.* 2007; Wang *et al.* 2020), and cancer prevention and treatment (Cheadle *et al.* 2017; Wang *et al.* 2021). For example, the imidazoquinoline analog R837 has been employed as an immune response modulating drug to treat viral infections (Miller *et al.* 1999). Isatoribine (ANA-245) has demonstrated potential in reducing viral load in hepatitis C patients (Fletcher *et al.* 2006). GS-9620 is another TLR7 agonist capable of suppressing the HBV in animal models of chronic infection (Bam *et al.* 2017). However, TLR7 agonists

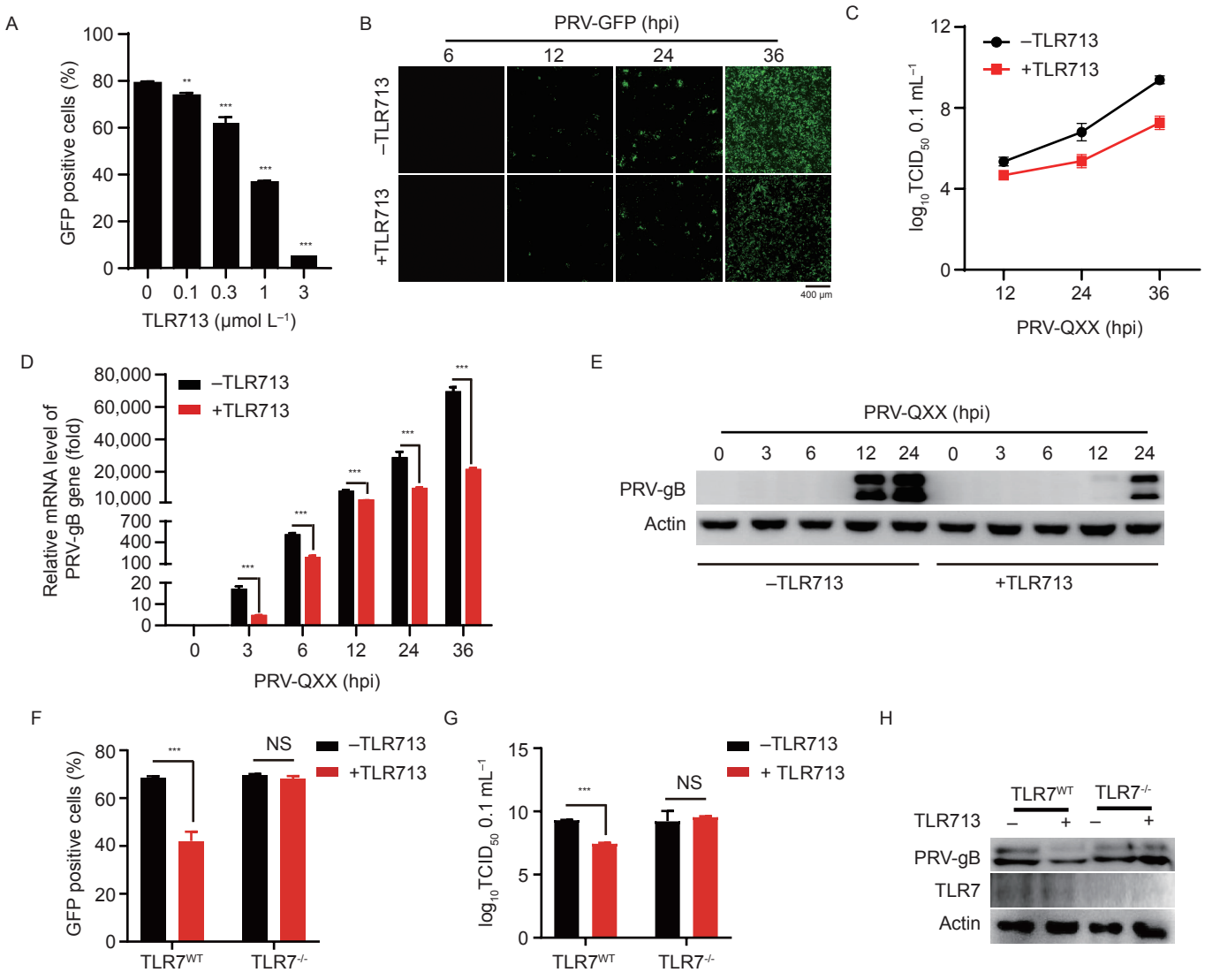


Fig. 3 TLR713 inhibits PRV proliferation through TLR7 pathway *in vitro*. A–C, PK-15 cells were infected with PRV-GFP (MOI=0.1), and treated with or without TLR713 (0–3 μmol L^{-1}) (A), 1 μmol L^{-1} (B and C) for 36 h. GFP-positive cells were analyzed by flow cytometry (A). Viral replication was analyzed by fluorescence microscopy (B). Viral titers were assessed by $TCID_{50}$ assay (C). D, PK-15 cells were treated as in C. mRNA level of *PRV-gB* gene was assessed by qRT-PCR analysis. E, PK-15 cells were treated as in C. Expression of *PRV-gB* was assessed by immunoblotting analysis. F and G, TLR7WT PK-15 cells and $TLR7^{-/-}$ PK-15 cells were infected with PRV-GFP (MOI=0.1), and treated with or without TLR713 (1 μmol L^{-1}) for 36 h. GFP-positive cells were analyzed by flow cytometry (F). Viral titers were assessed by $TCID_{50}$ assay (G). H, $TLR7^{WT}$ PK-15 cells and $TLR7^{-/-}$ PK-15 were treated as in G. Expression of PRV-gB was assessed by immunoblotting analysis. hpi, hours post infection. Data are mean±SD (*n*=3). **, *P*<0.01; ***, *P*<0.001; NS, no significance.

are small molecules characterized by rapid metabolism and narrow therapeutic windows, leading to inefficient and inconsistent results thus far (Hu *et al.* 2020).

In this study, we aimed to generate a novel TLR7 agonist that could be used as an antiviral agent. We synthesized a pyrrolo[3,2-*d*]pyrimidine derivative, TLR713, as a TLR7 agonist. Structural observations of known TLR7 agonists reveal several common aspects. Firstly, they all contain a polycyclic core scaffold, with at least a heteroaromatic ring. Secondly, a nitrogen hydrogen bond acceptor and an adjacent unsubstituted NH_2 hydrogen bond donor are contained in the core structure. Thirdly, a hydrophobic tail, has typically four carbon atoms and is connected to an oxygen or nitrogen atom which is positioned four bonds away from the aryl group (McGowan *et al.* 2017). The structure of TLR713 fits these criteria perfectly, indicating that TLR713 has great potential as a TLR7 agonist.

TLR7 signaling activation induces the expression of cytokines (such as TNF-α and IL-6) and type I interferon. A TLR7 agonist can effectively induce IL-6 production from monocytes (Song *et al.* 2021), and can lead to increased secretion of TNFα and IL-1β (Coleman *et al.* 2017). The TLR7 agonist 852A stimulates pDCs to secrete an abundance of type I IFN inhibiting the proliferation of tumor cells (Inglefield *et al.* 2008). TLR713 showed potent TLR7 activity in $TLR7^{WT}$ cells compared to $TLR7^{-/-}$ cells because we observed significant activity in inducing the expression of NF-κB-associated genes (e.g., *IL-6*, *IL-12*) and *ISG-15* in $TLR7^{WT}$

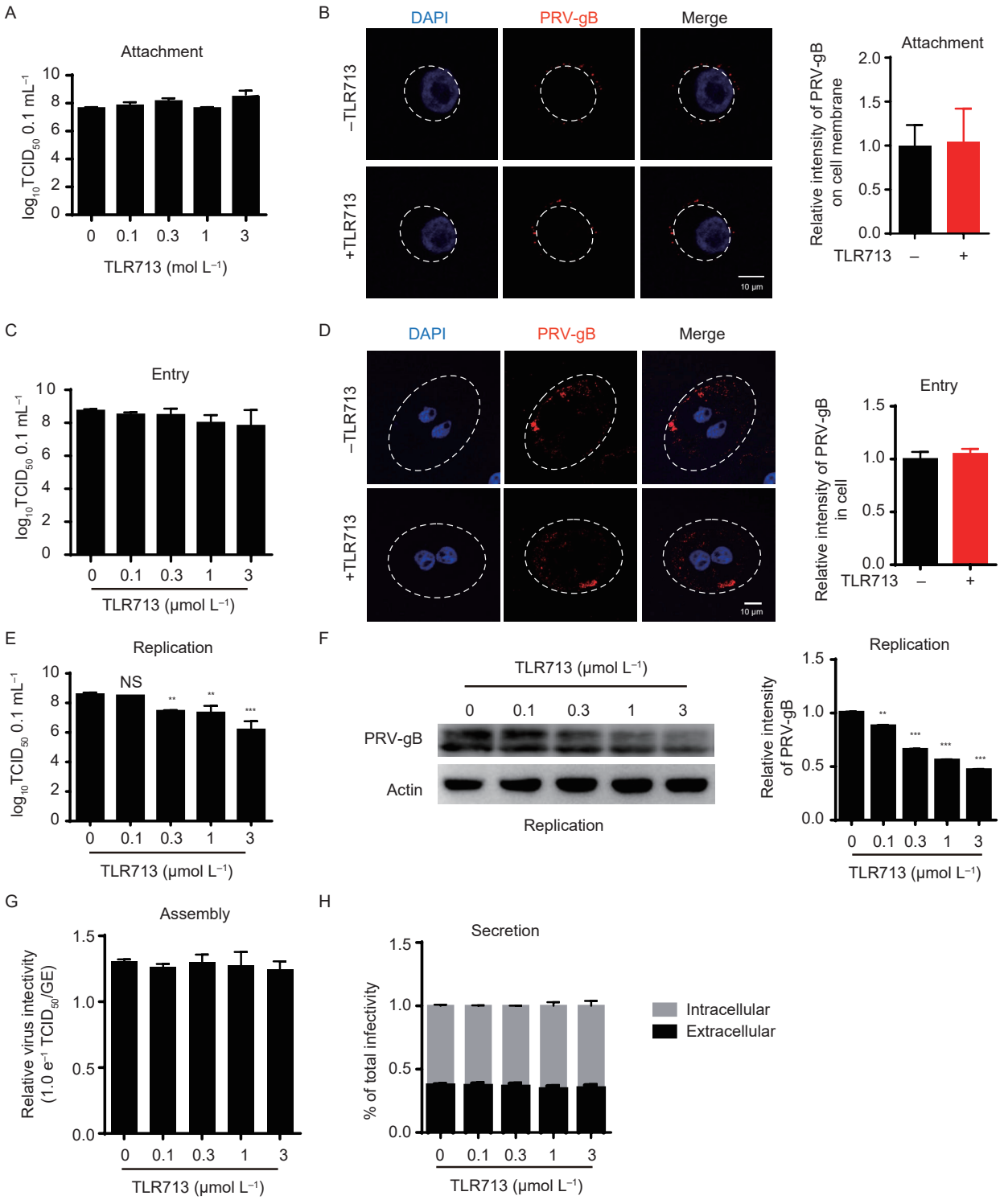


Fig. 4 TLR713 restricts PRV replication. A, PK-15 were incubated with PRV-QXX (MOI=0.1) with TLR713 (0–3 μmol L^{-1}) for 1 h on ice, cultured for another 24 h. Viral titers were assessed by $TCID_{50}$ assay. B, PK-15 were incubated with PRV-QXX (MOI=10) with TLR713 (0–3 μmol L^{-1}) for 1 h on ice, stained with antibodies against PRV-gB. Infected cells were highlighted by white dotted lines. C, PK-15 cells were incubated with PRV-QXX (MOI=0.1) for 1 h at 37°C, incubated with TLR713 (0–3 μmol L^{-1}) at 37°C for 30 min to allow entry, washed with trypsin (1 mg mL^{-1}), cultured for another 24 h. Viral titers were assessed by $TCID_{50}$ assay. D, PK-15 cells were incubated with PRV-QXX (MOI=10) for 1 h at 37°C, incubated with TLR713 (0–3 μmol L^{-1}) at 37°C for 30 min, stained with antibodies against PRV-gB. Infected cells were highlighted by white dotted lines. E, PK-15 cells were incubated with PRV-QXX (MOI=0.1) for 1 h at 37°C, cultured with TLR713 (0–3 μmol L^{-1}) at 37°C for 24 h. Viral titers were assessed by $TCID_{50}$ assay. F, PK-15 cells were infected with PRV-QXX as in E. Expression of PRV-gB were assessed by immunoblotting analysis. G, efficiency of viral assembly was determined by the ratio of the virus titer to the total PRV genome. Copy numbers of the PRV genome were assayed by qRT-PCR. H, efficiency of viral secretion was determined by the ratio of intra- and extracellular infectivity relative to total infectivity. PK-15 cells were infected with PRV-QXX as in E. Infectivity of viral in supernatants and cells were determined by $TCID_{50}$ assay. Data are mean±SD (n=4) **, P<0.01; ***, P<0.001; NS, no significance.

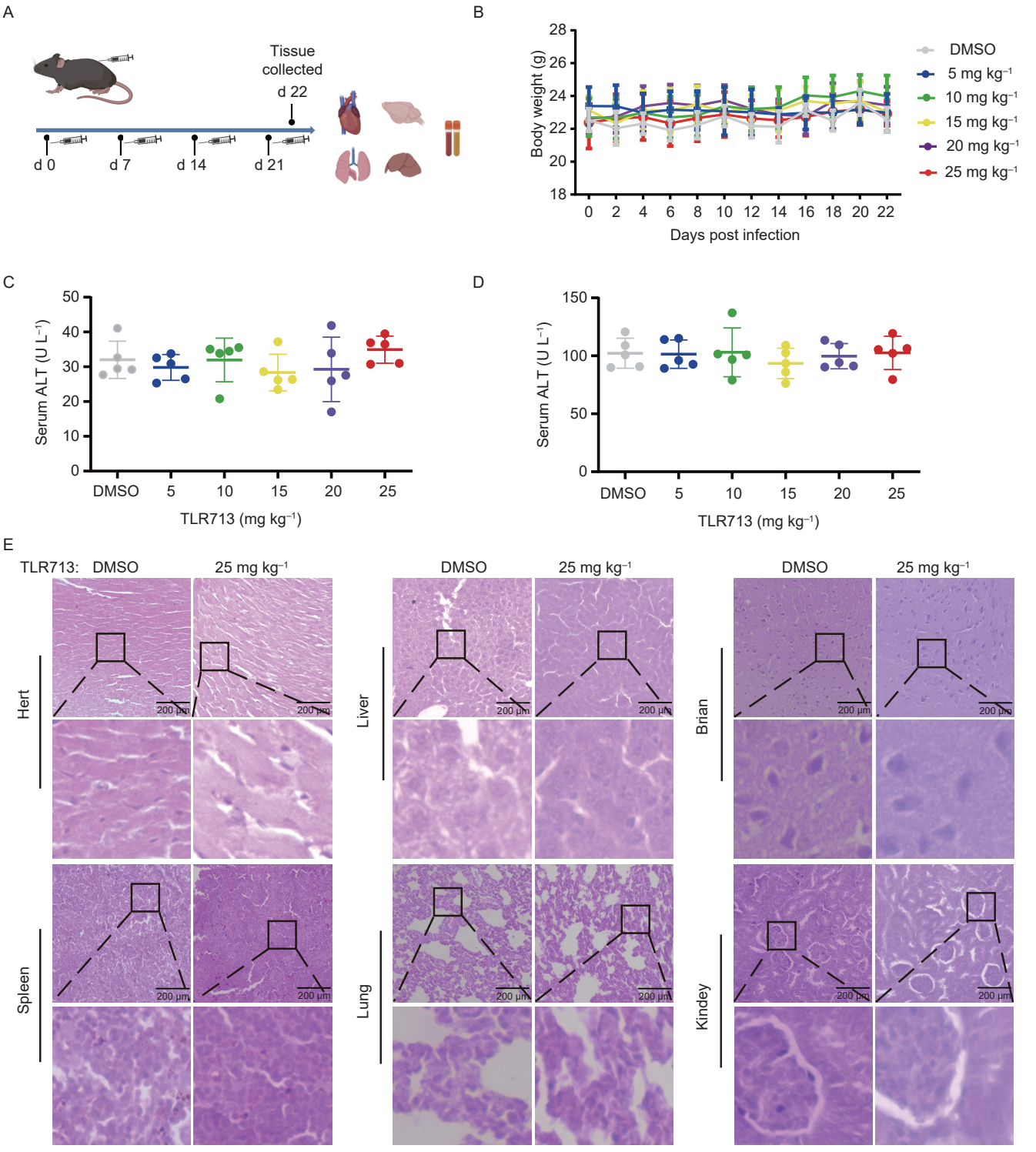


Fig. 5 TLR713 does not produce adverse side effects *in vivo*. A, 8-wk-old female C57BL/6 mice (n=6 per group) were injected S.C. (subcutaneous) weekly with TLR713 (0–25 mg kg^{-1}) 4 times. At d 22, terminal blood samples and tissues were harvested. B, averaged weights of the mice in each group. C and D, at d 22, terminal blood samples were collected and the activity of serum ALT and AST was measured. E, at d 22, tissues were harvested for H&E stain. ALT, alanine aminotransferase; AST, aspartate aminotransferase. Data are mean±SD (n=5).

cells.

We used PRV to evaluate the antiviral activity of TLR713. The results demonstrated that TLR713 can inhibit PRV replication *via* TLR7. To explore the mechanism by which TLR713 inhibits PRV replication, we investigated the effect of TLR713 on the PRV lifecycle. The results indicated that TLR713 did not directly kill the virus (data not shown), nor did it affect the entry, attachment, assembly, of secretion stages of the lifecycle. However, TLR713 did impact the replication process of PRV. The release of inflammatory cytokines, such

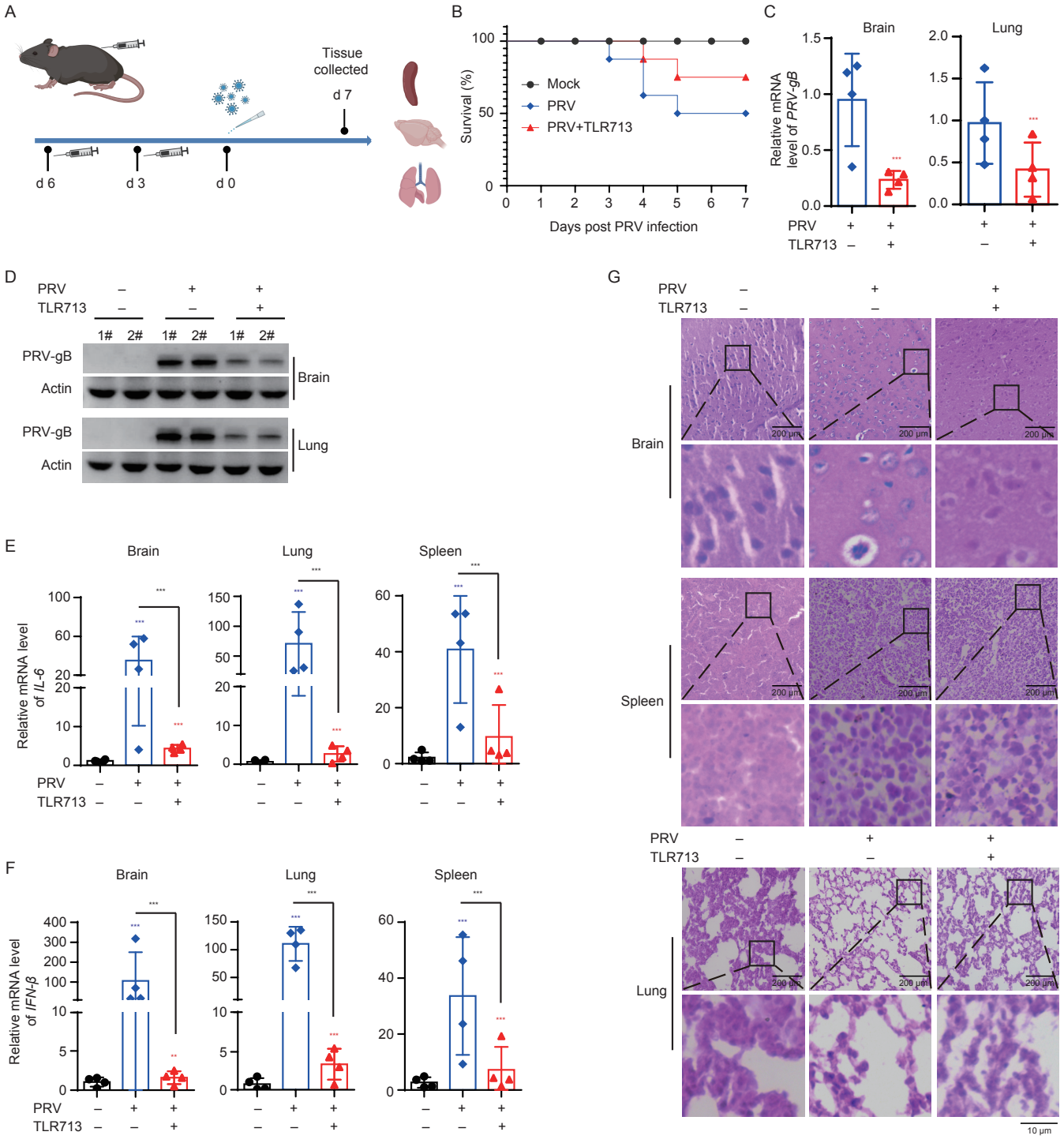


Fig. 6 TLR713 protects mice against PRV infection. A, female 8-wk-old C57BL/6 mice (n=8) were injected S.C. (subcutaneous) twice with TLR713 (5 mg kg^{-1}) before infected with PRV-QXX (LD_{50}, 1×10^3 $TCID_{50}$) through nasal intubation drip. On d 7 post infection, the survival mice were sacrificed, and tissues were collected. B, survival rate of mice after infected with PRV-QXX was recorded daily. C, relative mRNA level of *PRV-gB* gene in brain and lung were detected by qRT-PCR analysis. D, expression of PRV-gB in brain and lung were assessed by immunoblotting analysis. E and F, relative mRNA levels of *IL-6* and *IFN-β* gene in brain, lung, and spleen were detected by qRT-PCR analysis. G, representative micrographs of H&E stained sections. LD_{50}, the median lethal dose. Data are mean±SD (n=4) ***, P<0.001.

as IL-1β and IL-6, is critical for controlling PRV replication (Ye *et al.* 2021; Zhou *et al.* 2023). To determine whether cytokines induced by TLR713 inhibited PRV replication, supernatants from PK-15 and 3D4/21 cells stimulated with TLR713 were collected and added to PK-15 cells infected with PRV. The results showed that PRV-GFP infection in PK-15 cells was significantly inhibited when treated with supernatants from TLR713-treated PK-15 and 3D4/21 cells (data not shown).

Normally, TLR7 agonists exert an antiviral effect by

activating innate immunity and inducing the release of cytokines. Loxoribine, a guanosine ribonucleoside analogue, activates TLR7. This compound exhibits antiviral activity by activating NK and B cells to induce multiple cytokines (Gosu *et al.* 2012). Isatoribine and GS-9620 also exhibit antiviral activity by inducing multiple cytokines (Thomas *et al.* 2007; Enosi Tuipulotu *et al.* 2018). The types of these cytokines include, but are not limited to, interleukins, IFNs, and ISGs. These cytokines may be one reason why TLR713 exerts its antiviral effect. Further research is needed to explore the key steps by which TLR713 inhibits PRV infection, which could provide valuable insights for the development of antiviral agents.

5. Conclusion

In this study, we report on a pyrrolo[3,2-*d*]pyrimidine derivative that exhibits anti-PRV effects both in vitro and in vivo. Specifically, it inhibits PRV replication but does not affect viral attachment, entry, assembly or release by targeting TLR7.

Acknowledgements

This work was financially supported by the Key R&D Special Project of Henan Province, China (241111110300), the National Natural Science Foundation of China (32402849), the Department of Henan Science and Technology, China (252102110035), the Doctoral Research Initiation Fund of Henan University of Animal Husbandry and Economy, China (2022HNUAHEDF033), and Key Research Projects of Higher Education Institutions in Henan Province, China (25A150025).

Declaration of competing interest

The authors declare that they have no conflict of interest.

Declaration of generative AI and AI-assisted technologies in the writing process

The authors declare that they did not use AI in the preparation and writing of this manuscript.

Ethical approval

All animals experiments were approved by the Guide for the Care and Use of Laboratory Animals, and the related ethical regulations instilled at Henan Agricultural University. All institutional and national guidelines for the care and use of laboratory animals were followed.

Appendix associated with this study is available at https://doi.org/10.1016/j.jia.2024.07.001

References

Bam R A, Hansen D, Irrinki A, Mulato A, Jones G S, Hesselgesser J, Frey C R, Cihlar T, Yant S R. 2017. TLR7 Agonist GS-9620 is a potent inhibitor of acute HIV-1 infection in human peripheral blood mononuclear cells. *Antimicrobial Agents and Chemotherapy*, **61**, 1369–1316.

Cheadle E J, Lipowska-Bhalla G, Dovedi S J, Fagnano E, Klein C, Honeychurch J, Illidge T M. 2017. A TLR7 agonist enhances the antitumor efficacy of obinutuzumab in murine lymphoma models *via* NK cells and CD4 T cells. *Leukemia*, **31**, 1611–1621.

Coleman L G J, Zou J, Crews F T. 2017. Microglial-derived miRNA let-7 and HMGB1 contribute to ethanol-induced neurotoxicity *via* TLR7. *Journal of Neuroinflammation*, **14**, 22–33.

Das D, Sengupta I, Sarkar N, Pal A, Saha D, Bandopadhyay M, Das C, Narayan J, Singh S P, Chakrabarti S, Chakravarty R. 2017. Anti-hepatitis B virus (HBV) response of imiquimod based toll like receptor 7 ligand in hbv-positive human hepatocelluar carcinoma cell line. *BMC Infectious Disease*, **17**, 76–87.

Enosi Tuipulotu D, Netzler N E, Lun J H, Mackenzie J M, White P A. 2018. TLR7 agonists display potent antiviral effects against norovirus infection *via* innate stimulation. *Antimicrob Agents Chemother*, **62**, e02417–17.

Fernandes-Santos C, Azeredo E L. 2022. Innate immune response to dengue virus: Toll-like receptors and antiviral response. *Viruses*, **14**, 992.

Fletcher S, Steffy K, Averett D. 2006. Masked oral prodrugs of toll-like receptor 7 agonists: A new approach for the treatment of infectious disease. *Current Opinion in Investigational Drugs*, **7**, 702–708.

Gosu V, Basith S, Kwon O P, Choi S. 2012. Therapeutic applications of nucleic acids and their analogues in toll-like receptor signaling. *Molecules*, **17**, 13503–13529.

Gotovtseva E P, Kapadia A S, Smolensky M H, Lairson D R. 2008. Optimal frequency of imiquimod (aldara) 5% cream for the treatment of external genital warts in immunocompetent adults: A meta-analysis. *Sexually Transmitted Diseases*, **35**, 346–351.

Guo Y K, Ming S L, Zeng L, Chang W R, Pan J J, Zhang C, Wan B, Wang J, Su Y, Yang G Y, Chu B B. 2021. Inhibition of histone deacetylase 1 suppresses pseudorabies virus infection through cGAS-STING antiviral innate immunity. *Molecular Immunology*, **136**, 55–64.

Herschke F, Li C, Zhu R, Han Q, Wu Q, Lu Q, Barale-Thomas E, Jonghe S D, Lin T I, An D C. 2021. JNJ-64794964 (AL-034/TQ-A3334), a TLR7 agonist, induces sustained anti-HBV activity in AAV/HBV mice *via* non-cytolytic mechanisms. *Antiviral Research*, **196**, 105196.

Hu Y, Tang L, Zhu Z, Meng H, Chen T, Zhao S, Jin Z, Wang Z, Jin G. 2020. A novel TLR7 agonist as adjuvant to stimulate high quality HBsAg-specific immune responses in an HBV mouse model. *Journal of Translational Medicine*, **18**, 112–125.

Inglefield J R, Dumitru C D, Alkan S S, Gibson S J, Lipson K E, Tomai M A, Larson C J, Vasilakos J P. 2008. TLR7 agonist 852A inhibition of tumor cell proliferation is dependent on plasmacytoid dendritic cells and type I IFN. *Journal of Interferon Cytokine Research*, **28**, 253–263.

Jahanban-Esfahlan R, Seidi K, Majidinia M, Karimian A, Yousefi B, Nabavi S M, Astani A, Berindan-Neagoe I, Gulei D, Fallarino F, Gargaro M, Manni G, Pirro M, Xu S, Sadeghi M, Nabavi S F, Shirooie S. 2019. Toll-like receptors as novel therapeutic targets for herpes simplex virus infection. *Reviews in Medical Virology*, **29**, e2048.

Janovec V, Hodek J, Clarova K, Hofman T, Dostalik P, Fronek J, Chlupac J, Chaperot L, Durand S, Baumert T F, Pichova I, Lubyova B, Hirsch I, Weber J. 2020. Toll-like receptor dual-acting agonists are potent inducers of PBMC-produced cytokines that inhibit hepatitis B virus production in primary human hepatocytes. *Scientific Reports*, **10**, 12767.

Kanneganti T D, Ozoren N, Body-Malapel M, Amer A, Park J H, Franchi L, Whitfield J, Barchet W, Colonna M, Vandenabeele P, Bertin J, Coyle A, Grant E P, Akira S, Nunez G. 2006. Bacterial RNA and small antiviral compounds activate caspase-1 through cryopyrin/Nalp3. *Nature*, **440**, 233–236.

Koerner J, Horvath D, Herrmann V L, MacKerracher A, Gander B, Yagita H, Rohayem J, Groettrup M. 2021. PLGA-particle vaccine carrying TLR3/RIG-I ligand Riboxxim synergizes with immune checkpoint blockade for effective anti-cancer immunotherapy. *Nature Communications*, **12**, 2935.

Lucifora J, Bonnin M, Aillot L, Fusil F, Maadadi S, Dimier L, Michelet M, Floriot O, Ollivier A, Rivoire M, Ait-Goughoulte M, Daffis S, Fletcher S P, Salvetti A, Cosset F L, Zoulim F, Durantel D. 2018. Direct antiviral properties of TLR ligands against HBV replication in immune-competent hepatocytes. *Scientific Reports*, **8**, 5390.

Mark K, Corey L, Meng T, Magaret A, Huang M, Selke S, Slade H, Tyring S, Warren T, Sacks S, Leone P, Bergland V, Wald A. 2007. Topical resiquimod 0.01% gel decreases herpes simplex virus type 2 genital shedding: A randomized, controlled trial. *The Journal of Infectious Diseases*, **195**, 1324–1331.

McGowan D C, Herschke F, Pauwels F, Stoops B, Smyej I, Last S, Pieters S, Embrechts W, Khamlichi M D, Thone T, Van Schoubroeck

B, Mostmans W, Wuyts D, Verstappen D, Scholliers A, De Pooter D, Dhuyvetter D, Borghys H, Tuefferd M, Arnoult E, *et al.* 2017. Identification and optimization of Pyrrolo[3,2-d]pyrimidine toll-like receptor 7 (TLR7) selective agonists for the treatment of hepatitis B. *Journal of Medical Chemistry*, **60**, 6137–6151.

Meng J J, Song Y, Fan W, Yang L, Xing J, Wang J, Chu B, Yang G, Wang M. 2022. Effect of *Toll-like Receptor 7* gene knockout on pmliferation of vesicular stomatitis virus. *China Animal Husbandry & Veterinary Medicine*, **49**, 2011–2021. (in Chinese)

Menne S, Tumas D B, Liu K H, Thampi L, AlDeghaither D, Baldwin B H, Bellezza C A, Cote P J, Zheng J, Halcomb R, Fosdick A, Fletcher S P, Daffis S, Li L, Yue P, Wolfgang G H, Tennant B C. 2015. Sustained efficacy and seroconversion with the Toll-like receptor 7 agonist GS-9620 in the Woodchuck model of chronic hepatitis B. *Journal of Hepatology*, **62**, 1237–1245.

Mentrup T, Stumpff-Niggemann A Y, Leinung N, Schlosser C, Schubert K, Wehner R, Tunger A, Schatz V, Neubert P, Gradtke A C, Wolf J, Rose-John S, Saftig P, Dalpke A, Jantsch J, Schmitz M, Fluhrer R, Jacobsen I D, Schroder B. 2022. Phagosomal signalling of the C-type lectin receptor Dectin-1 is terminated by intramembrane proteolysis. *Nature Communications*, **13**, 1880.

Miller R, Gerster J, Owens M, Slade H, Tomai M. 1999. Imiquimod applied topically: A novel immune response modifier and new class of drug. *International Journal of Immunopharmacology*, **21**, 1–14.

Naqvi I, Giroux N, Olson L, Morrison S A, Llanga T, Akinade T O, Zhu Y, Zhong Y, Bose S, Arvai S, Abramson K, Chen L, Que L, Kraft B, Shen X, Lee J, Leong K W, Nair S K, Sullenger B. 2022. DAMPs/PAMPs induce monocytic TLR activation and tolerance in COVID-19 patients; nucleic acid binding scavengers can counteract such TLR agonists. *Biomaterials*, **283**, 121393.

Nishii N, Tachinami H, Kondo Y, Xia Y, Kashima Y, Ohno T, Nagai S, Li L, Lau W, Harada H, Azuma M. 2018. Systemic administration of a TLR7 agonist attenuates regulatory T cells by dendritic cell modification and overcomes resistance to PD-L1 blockade therapy. *Oncotarget*, **9**, 13301–13312.

Savidis G, McDougall W M, Meraner P, Perreira J M, Portmann J M, Trincucci G, John S P, Aker A M, Renzette N, Robbins D R, Guo Z, Green S, Kowalik T F, Brass A L. 2016. Identification of zika virus and dengue virus dependency factors using functional genomics. *Cell Reports*, **16**, 232–246.

Shao Y, Saredy J, Yang W Y, Sun Y, Lu Y, Saaoud F, Drummer C T, Johnson C, Xu K, Jiang X, Wang H, Yang X. 2020. Vascular endothelial cells and innate immunity. *Arteriosclerosis Thrombiosis and Vasculae Biology*, **40**, e138–e152.

Song R, Gao Y, Dozmorov I, Malladi V, Saha I, McDaniel M M, Parameswaran S, Liang C, Arana C, Zhang B, Wakeland B, Zhou J, Weirauch M T, Kottyan L C, Wakeland E K, Pasare C. 2021. IRF1 governs the differential interferon-stimulated gene responses in human monocytes and macrophages by regulating chromatin accessibility. *Cell Reports*, **34**, 108891.

Song Y, Fan W, Yao C, Wang H, Lu X, Wang Y, Liu P, Ma Y, Zhang Z, Wang J, Chu B, Shi L, Yang G, Wang M. 2024. Design, synthesis and biological evaluation of quinazoline and pyrrolo[3,2-*d*]pyrimidine derivatives as TLR7 agonists for antiviral agents. *Organic & Biomolecular Chemistry*, **22**, 2764–2773.

Takeda K, Akira S. 2004. TLR signaling pathways. *Seminars in Immunology*, **16**, 3–9.

Thomas A, Laxton C, Rodman J, Myangar N, Horscroft N, Parkinson T. 2007. Investigating Toll-like receptor agonists for potential to treat hepatitis C virus infection. *Antimicrobial Agents and Chemotherapy*, **51**, 2969–2978.

Tomai M, Miller R, Lipson K, Kieper W, Zarraga I, Vasilakos J. 2007. Resiquimod and other immune response modifiers as vaccine adjuvants. *Expert Review of Vaccines*, **6**, 835–847.

Vanwalscappel B, Tada T, Landau N R. 2018. Toll-like receptor agonist R848 blocks Zika virus replication by inducing the antiviral protein viperin. *Virology*, **522**, 199–208.

Wang J, Li G L, Ming S L, Wang C F, Shi L J, Su B Q, Wu H T, Zeng L, Han Y Q, Liu Z H, Jiang D W, Du Y K, Li X D, Zhang G P, Yang G Y, Chu B B. 2020. BRD4 inhibition exerts anti-viral activity through DNA damage-dependent innate immune responses. *PLoS Pathogen*, **16**, e1008429.

Wang Q, Zhou L, Wang J, Su D, Li D, Du Y, Yang G, Zhang G, Chu B. 2022. African swine fever virus K205R induces ER stress and consequently activates autophagy and the NF-κB signaling pathway. *Viruses*, **14**, 394.

Wang X, Yu B, Cao B, Zhou J, Deng Y, Wang Z, Jin G. 2021. A chemical conjugation of JQ-1 and a TLR7 agonist induces tumoricidal effects in a murine model of melanoma *via* enhanced immunomodulation. *International Journal of Cancer*, **148**, 437–447.

Xiao L, Liu Y, Wang N. 2014. New paradigms in inflammatory signaling in vascular endothelial cells. *American Journal of Physiology Heart and Circulatory Physiology*, **306**, 317–325.

Xun Y, Yang H, Kaminska B, You H. 2021. Toll-like receptors and toll-like receptor-targeted immunotherapy against glioma. *Journal of Hematology & Oncology*, **14**, 176–207.

Ye C, Huang Q, Jiang J, Li G, Xu D, Zeng Z, Peng L, Peng Y, Fang R. 2021. ATP-dependent activation of NLRP3 inflammasome in primary murine macrophages infected by pseudorabies virus. *Veterinary Microbiology*, **259**, 109130.

Yeh F, Chen C, Xie C, Baxan N, Zhao L, Ashek A, Sabrin F, Lawrie A, Wilkins M, Zhao L. 2023. TLR7/8 activation induces autoimmune vasculopathy and causes severe pulmonary arterial hypertension. *The European Respiratory Journal*, **62**, 2300204.

Zhang Z, Ohto U, Shibata T, Krayukhina E, Taoka M, Yamauchi Y, Tanji H, Isobe T, Uchiyama S, Miyake K, Shimizu T. 2016. Structural analysis reveals that toll-like receptor 7 is a dual receptor for guanosine and single-stranded RNA. *Immunity*, **45**, 737–748.

Zhou Q, Zhang L, Lin Q, Liu H, Ye G, Liu X, Jiao S, Li J, Tang Y, Shi D, Huang L, Weng C. 2023. Pseudorabies virus infection activates the TLR-NF-κB axis and AIM2 inflammasome to enhance inflammatory responses in mice. *Journal of Virology*, **97**, e0000323.

Executive Editor-in-Chief Dongming Zhao
Managing Editor Han Zhang